FLUCOME 2009
10th International Conference on Fluid Control, Measurements, and Visualization
August 17–21, 2009, Moscow, Russia

IMPINGEMENT OF UNDEREXPANDED JET ON CONE

Ryota Seryu[1] and Junjiro Iwamoto[2]

ABSTRACT

When an underexpanded jet impinges on an object, some interesting phenomena can occur in the flow field, as can be found in cooling jet of the industrial process, exhaust jet of rocket engine and so on. For example, it is known that geometry and location of shock wave formed in front of the object vary with operating conditions of jet. In this study, to obtain a detailed flow pattern of flow field where the underexpanded jet issuing from a convergent nozzle impinges on the cone, the density distribution is obtained by applying the Mach-Zehnder interferometry and the pressure distribution on the cone surface is measured with pressure taps in the experiment. As a result, it is found that depending on the vertex location in the cell structure of the free jet, the geometry and location of shock and the structure of the jet along the cone are changed, and thus, the flow pattern including the density distribution in the flow field and the pressure distribution on the cone surface are changed.

Keywords: Shock Wave, Supersonic Flow, Underexpanded Jet, Impinging Jet, Cone

INTRODUCTION

The jet discharged from a convergent nozzle when the pressure ratio across the convergent nozzle (*NPR*) is higher than the critical pressure ratio becomes underexpanded. It is well-known that this jet has the barrel-shaped cellular structure which consists of the expansion region and the compression region. Depending on operating conditions, an oblique shock wave forms in the compression region and at high *NPR* the normal shock wave known as Mach disk occurs. For such a jet, it is reported that interesting phenomena such as jet oscillation (Panda, 1998) or jet noise characteristic of supersonic, involving screech tone (Tam, 1995), may occur.

When the jet impinges on an object, as can be found in cooling jet of the industrial process, exhaust jet of rocket engine and so on, some interesting phenomena can occur in the flow field. For example, it is known that geometry and location of shock wave formed in front of the object vary with operating conditions of jet and its shape (Iwamoto, 1990). The flow field where the underexpanded jet impinges on the object has been studied by many researchers, but the most of the object used so far is flat plate (Nakamura & Iwamoto, 2000) or wedge (Lamont & Hunt, 1976). Thus, it is desired that the flow field formed by the jet impinging on the objects having various shapes is examined. On the other hand, concerning impingement of jet on the object of general three-dimensional shape, the flow field is very

[1] Graduate School of Engineering, Tokyo Denki University, 2-2 Kanda-Nishiki-cho, Chiyoda-ku, Tokyo 101-8457, Japan, e-mail: 08gmm16@ms.dendai.ac.jp

[2] Department of Mechanical Engineering, Tokyo Denki University, 2-2 Kanda-Nishiki-cho, Chiyoda-ku, Tokyo 101-8457, Japan, e-mail: iwamoto@cck.dendai.ac.jp

complicated. The flow patterns obtained for the objects of simple geometry such as flat plate, cone, wedge etc. are most important to be established in the first place. In the present study the cone is used for the object of impingement because it has not been well studied yet so far.

In order to obtain a detailed flow pattern of a flow field where the underexpanded jet impinges on the cone, the density distribution is obtained by applying Mach-Zehnder interferometry and pressure distribution on the cone surface is measured with pressure taps in the experiment.

EXPERIMENTAL APPARATUS AND METHODOLOGY

Experimental Apparatus

The apparatus used is shown schematically in Fig. 1. In this study, working fluid is air. High-pressure air generated by two compressors is supplied into the plenum tank fitted with a convergent nozzle through an air dryer, a surge tank, an oil removal filter and an oil mist separator. The air is discharged into the atmosphere in sound-proof room, and the jet from the convergent nozzle impinges on the cone attached to a traversing mechanism. The stagnation pressure in the plenum tank is measured by a digital manometer and adjusted manually by a control valve on a pipe line.

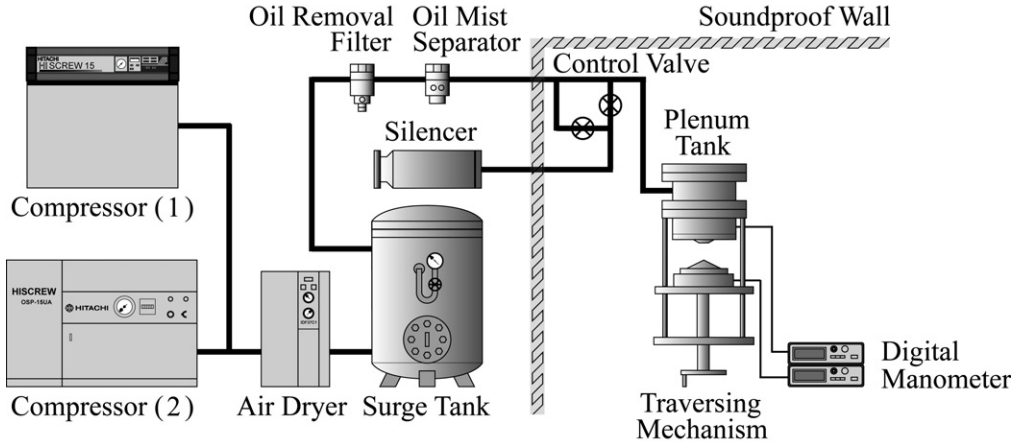

Fig. 1. Experimental apparatus

Experimental Conditions and Parameters

The convergent nozzle and a coordinate system in this study are shown schematically in Fig. 2. The exit diameter D is 10 mm and the radius of curvature of its inner wall being 20 mm. The surface of the inner wall of the nozzle is well finished. Experimental parameters are the ratio of stagnation pressure in the plenum tank to ambient pressure NPR, nozzle-to-cone distance l/D, and the vertex angle θ. In the present study, NPR is changed from 2.0 to 4.0 with 0.5 steps, l/D from 0.0 to 2.0 with 0.1 steps and the cones whose angles are 60 deg and 120 deg are used.

Density Measurement by Mach-Zehnder Interferometry

The Mach-Zehnder interferometry is used to obtain density distribution of the flow field quantitatively. The arrangement of the optical system is shown in Fig. 3. A laser diode of wavelength 650 nm is used for a source of light which emits light synchronized to a signal of 10 kHz with duty ratio 50% from a pulse generator, i.e. a duration time of 50 μs. The finite fringe mode of Mach-Zehnder interferometry is used to

get more detailed density distribution, and fringes of the interferograms obtained by experiment are binarised and thinned by computer. In order to estimate the density distribution by the fringe shift of interferograms, it is assumed that the flow field is axisymmetric. Then, assuming that the density in each jet section normal to the jet axis divided into a series of concentric circles is constant, the density distribution may be obtained (Ladenburg, Winckler & Van Voorhis, 1948). In this study, the width of each circles are very small (less than 0.03mm), and the fringe shift between fringes is interpolated linearly.

Pressure Measurement by Pressure Tap

The pressure taps are used for the measurement of the pressure distributions along the cone surface. The diameters of pressure taps for the cones of 60 deg and 120 deg are 0.75 mm and 0.50 mm, respectively.

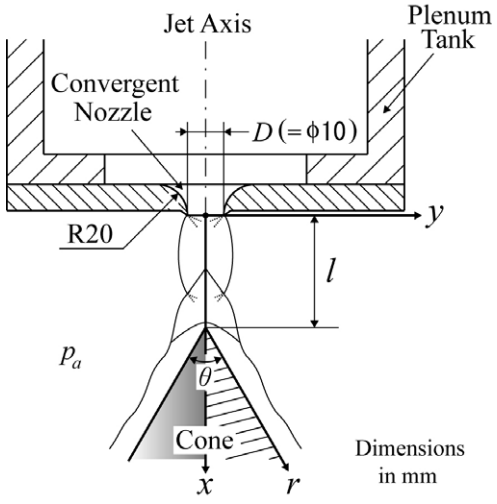

Fig. 2. Coordinate system

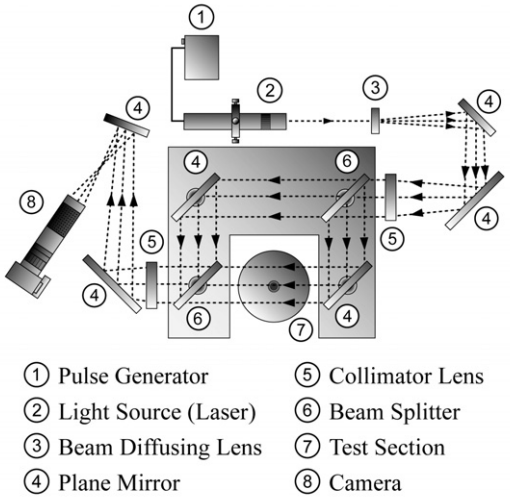

Fig. 3. The arrangement of the optical system

RESULTS AND DISCUSSION

Free Jet

The density distribution of the free jet is obtained by Mach-Zehnder interferometry and it is shown in Fig. 4, at *NPR* = 3.5. Figure 4(a) indicates an interferogram of thinned fringes. Since the flow field is axisymmetric, only a half of the field is shown, the jet axis being on the left in the figure. Figure 4(b) shows the density distribution estimated from the interferogram in Fig. 4(a), using the above-mentioned method. As shown, the flow pattern of a typical underexpanded jet is obtained, where the expansion wave generated at the nozzle lip propagates downstream, being reflected from the jet boundary as compression wave. The reflections of waves are repeated downstream, resulting in well known cellular structure of the jet.

It is reported that, for the jets impinging on the cone produced by the C-D nozzle with the exit Mach number of 2.2 and operating with ratios of nozzle lip pressure to ambient pressure of 1, 1.2 and 2, the most striking feature of this flow field is the shock pattern produced by the interaction between the cone shock and the jet shock, this pattern can take a wide variety of forms depending on the structure of the free jet and strongly influences the form of the cone surface pressure distribution (Jennions & Hunt, 1980).

Therefore, the flow pattern in this study is influenced by the relationship between the waves forming the shock cell structure of the underexpanded jet and the effect of the existence of the cone on the flow field. In order to clarify this, the jet is divided into six regions as follows;

(Ⅰ) : nozzle exit plane
(Ⅱ) : expansion region in the first cell
(Ⅲ) : flow area between expansion and compression region in the first cell
(Ⅳ) : compression region in the first cell
(Ⅴ) : boundary between first and second cell
(Ⅵ) : expansion region in the second cell

and they are shown in Fig. 4(b). In the present study, the flow characteristics are discussed using the density distributions of the impinging jet and the pressure measurements on the surface of the cone when the vertex of the cone is located in these regions shown above.

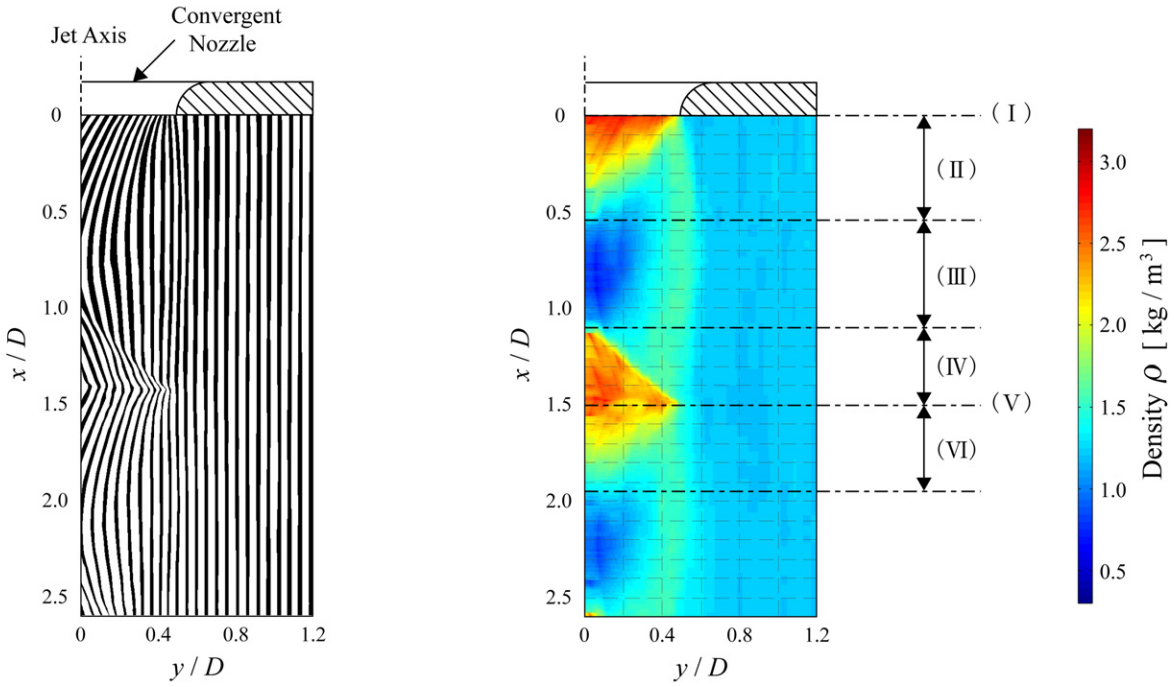

(a) Interferogram **(b) Density distribution**

Fig. 4. Density distribution of the free jet obtained by MZI at *NPR* = 3.5

Impingement of the Jet on Cone at *NPR* = 3.5 for θ = 60 deg

Figure 5 shows the density distributions obtained from the interferograms (left side) and the corresponding pressure distributions on the cone (right side) at *NPR* = 3.5 for θ = 60 deg. The density distributions in only one half of the flow field are shown since the flow is assumed to be axisymmetric.

As shown in Fig. 5(a), when the vertex of the cone is located at the nozzle exit plane l/D = 0.0 (region (Ⅰ), Fig. 4(b)), the density is high in the neighborhood of the vertex. The periodic pressure change can be seen along cone surface. The similar flow pattern is obtained at l/D = 0.1 and it changes dramatically at l/D = 0.2 (not shown in the figure).

At l/D = 0.3 where the vertex is located in the region (Ⅱ) in Fig. 4(b) the shock wave is attached to the vertex and is of bow type. Along the cone surface other shock waves can be seen, which are present due to the non-uniform nature of the supersonic jet flow.

When the cone is moved further downstream to l/D = 0.4 to 0.7, the shock attached to the cone also moves. On the other hand, the downstream shock does not move irrespective of the movement of the cone, thus resulting in the interaction of the downstream shock with the shock attached to the cone.

When the vertex of the cone is located at l/D = 0.8 in the region (Ⅲ), only a single shock forms in the flow field as shown in Fig. 5(c) and there is only small pressure change on the cone surface. As the nozzle-cone distance increases from l/D = 0.9 to 1.2, the distance between the vertex and the shock increases.

At l/D = 1.3 where the vertex of the cone is located in the region (Ⅳ) in Fig. 4(b), the shock is now a little away from the vertex and the density behind it is high. On the other hand, the pressure change on the cone surface is spatially periodic again, similar to that in Fig. 5(b), although its amplitude is much less.

In Fig. 5(e) where the vertex is located at the boundary between first and second cell in the region (Ⅴ), or at l/D = 1.5, the shock wave which stands in front of the cone is the one in the free jet. The pressure distribution on the cone surface is almost flat downstream of the area of gradual decrease in pressure from that at the vertex.

Figure 5(f) shows the flow pattern when the vertex is located at l/D = 1.7 in the region (Ⅵ) which is the expansion region of the second cell of the jet. It seems that the flow pattern downstream of the first cell structure in Fig. 5(f) is similar to that in Fig. 5(b). This suggests that the similar pattern of the flow field for θ = 60 deg may be presumed to be repeated downstream of the second cell.

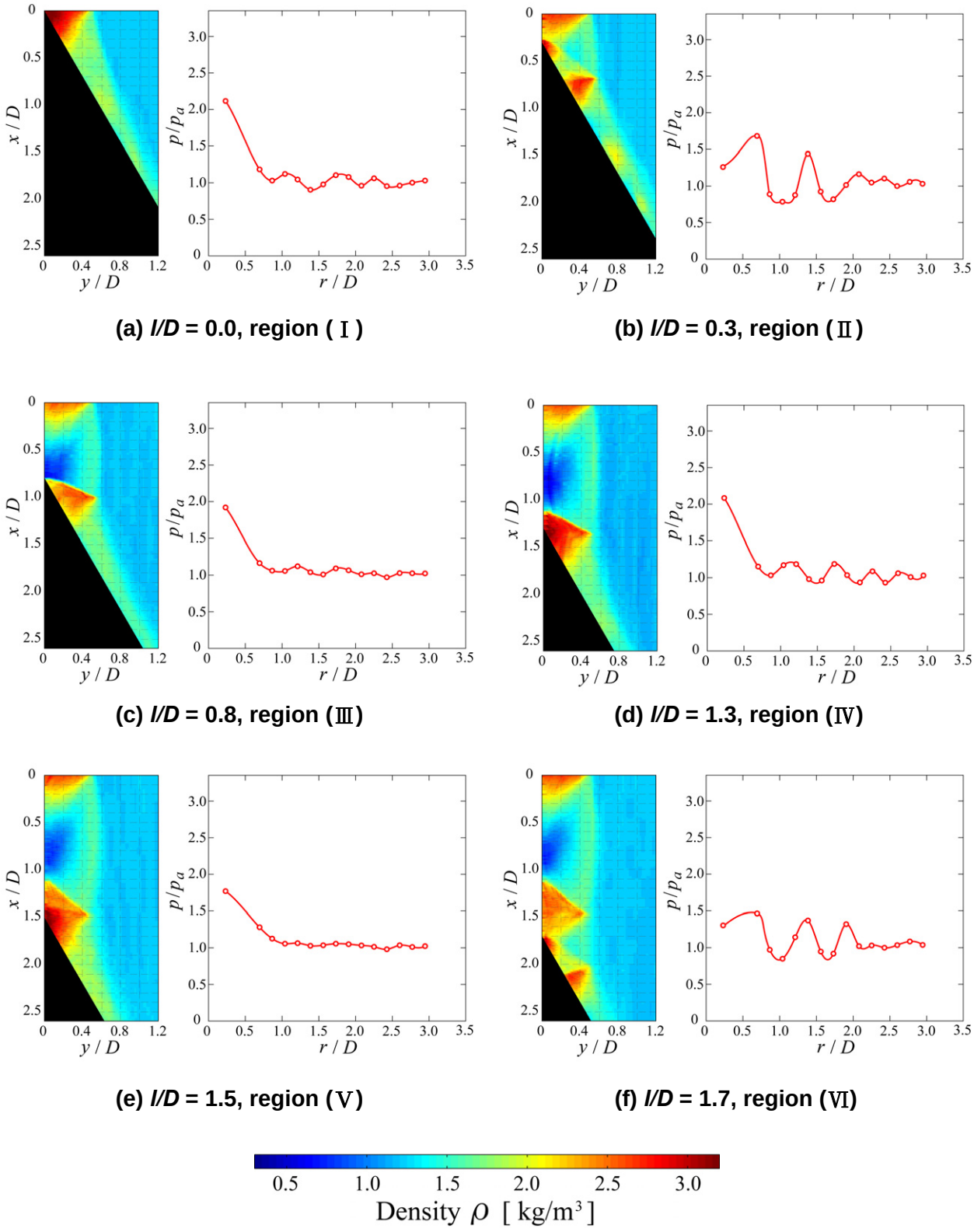

(a) *l/D* = 0.0, region (Ⅰ) **(b) *l/D* = 0.3, region (Ⅱ)**

(c) *l/D* = 0.8, region (Ⅲ) **(d) *l/D* = 1.3, region (Ⅳ)**

(e) *l/D* = 1.5, region (Ⅴ) **(f) *l/D* = 1.7, region (Ⅵ)**

Fig. 5. The density distributions obtained from interferograms (left side) and the pressure distributions on cone (right side) at *NPR* = 3.5 for *θ* = 60 deg

Impingement of the Jet on Cone at *NPR* = 3.5 for θ = 120 deg

Figure 6 shows the density distributions obtained from the interferograms (left side) and the corresponding pressure distributions on the cone (right side) at *NPR* = 3.5 for θ = 120 deg.

As shown in Fig. 6(a), when the vertex of the cone is located at the nozzle exit plane *l*/*D* = 0.0 (region (Ⅰ), Fig. 4(b)), the density is high in the neighborhood of the vertex and the pressure on the cone surface changes periodically, its amplitude being higher than that for θ = 60 deg.

When the vertex is located at *l*/*D* = 0.3 in the expansion region (Ⅱ), a bow shock forms in front of the cone. There is some pressure change on the cone surface. As the nozzle-cone distance *l*/*D* increases, the detached shock becomes flat in shape and this continues up to *l*/*D* = 0.5 which is close to the boundary between region (Ⅱ) and region (Ⅲ) in Fig. 4(b). When the nozzle-cone distance increases over *l*/*D* = 0.5, the shock wave becomes bow in shape again and detached gradually. Under these flow situations the pressure distributions on cone surface are similar to those in Fig. 6(b), and their amplitudes are smaller.

When the vertex is located at *l*/*D* = 0.8 in the region (Ⅲ), as shown in Fig. 6(c), the shock wave is bow in shape, and the pressure distribution on the cone surface is similar to that in Fig. 6(b), its amplitude being much smaller. As the cone is moved further downstream in the jet, this pressure distribution changes from that in Fig. 6(c) to that in Fig. 6(d), a relatively large change being at about *l*/*D* = 1.0 which is the end of the region (Ⅲ) in Fig. 4(b).

At *l*/*D* = 1.3 when the vertex is in the region (Ⅳ) the shock wave is more detached and the shape of the shock is like that in free jet, but is high curvature in the vicinity of the center as shown in Fig. 6(d). It is also observed that the successive density fluctuation occurs in the area close to the jet boundary. For flat plate, the similar flow pattern is known to exist and this consists of the reflection on the expansion and compression waves in narrow space between the jet boundary and the sonic line (Henderson, 2002).

When the vertex is located at *l*/*D* = 1.5 at the boundary between first and second cell (region (Ⅴ), in Fig. 4(b)) in Fig. 6(e), the shock stands further upstream. The pressure distribution on the cone is very similar to that in Fig. 6(d). With further increase in *l*/*D* = 1.5, the distance between the shock and the vertex of the cone increases up to *l*/*D* = 1.6.

When *l*/*D* = 1.7, the entire flow pattern in the neighborhood of the vertex changes dramatically as shown in Fig. 6(f); the oblique shock wave originally formed in the free jet occurs and the first cell becomes that of the free jet. As the cone moves from *l*/*D* = 1.5 to 1.7, the pressure distribution changes from that in Fig. 6(e) to Fig. 6(f). This sudden change takes place somewhere between *l*/*D* = 1.5 and 1.6, that is, between region (Ⅳ) or region (Ⅴ) and region (Ⅵ) in Fig. 4(b). The pressure distribution on the cone surface as shown in Fig. 6(f) remains almost the same up to *l*/*D* = 2.0.

When *l*/*D* = 1.8, where the vertex of the cone is located in the expansion region of the second cell, the flow pattern downstream of the first cell is similar to that in Fig. 6(b) where the vertex is placed in the expansion region of the first cell (not shown in the figure).

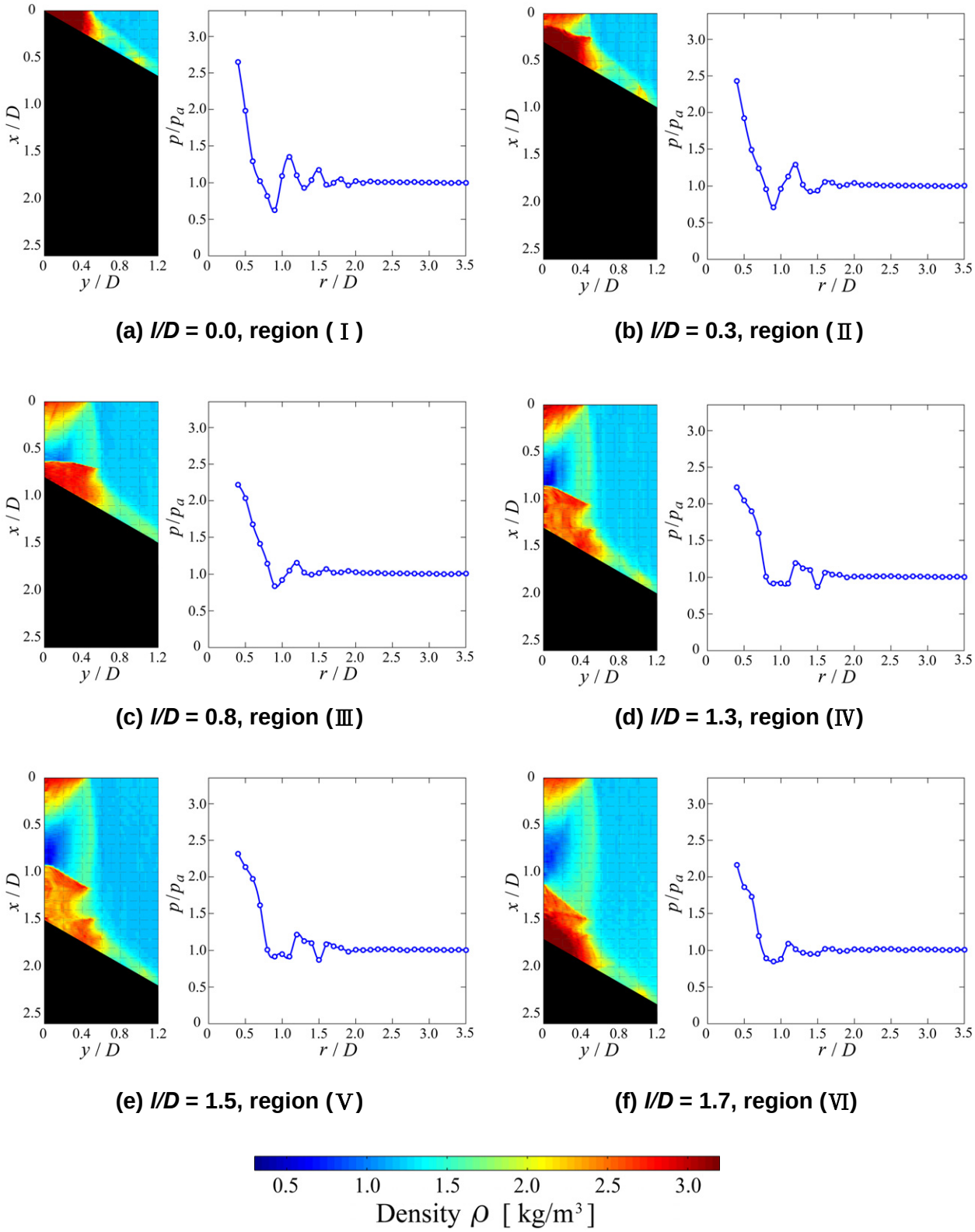

(a) *l/D* = 0.0, region (Ⅰ) **(b) *l/D* = 0.3, region (Ⅱ)**

(c) *l/D* = 0.8, region (Ⅲ) **(d) *l/D* = 1.3, region (Ⅳ)**

(e) *l/D* = 1.5, region (Ⅴ) **(f) *l/D* = 1.7, region (Ⅵ)**

Fig. 6. The density distributions obtained from interferograms (left side) and the pressure distributions on cone (right side) at *NPR* = 3.5 for *θ* = 120 deg

Impingement of the Jet on Cone at *NPR* = 4.0 in comparison with *NPR* = 3.5

Figures 7(a) and 7(b) show the density distributions obtained from the interferograms (left side) and the corresponding pressure distributions on the cone (right side) at *NPR* = 4.0 with *l*/*D* = 1.7 for θ = 60 deg and 120 deg, respectively.

The free jet at *NPR* = 4.0 has a normal shock wave known as Mach disk, whose appearance is one of the significant differences from that at *NPR* = 3.5. Therefore, it is easily presumed that the Mach disk may change the flow pattern downstream of it even at the same *l*/*D*.

At θ = 60 deg the density near the vertex in Fig. 7(a) is not so high as that at *NPR* = 3.5 in Fig. 5(f). It is considered that one of the factors to cause this phenomenon is that the shock is not formed in front of the vertex or the shock is very weak even if it is present because the flow is subsonic just behind the Mach disk. In addition, due to the higher *NPR* the amplitude of the pressure change on the cone surface is larger. Generally, overall flow patterns are qualitatively similar.

On the other hand, at θ = 120 deg, it is observed that the flow pattern shown in Fig. 7(b) is quite different from that in Fig. 6(f). In Fig. 7(b) the flow near the vertex can be divided into subsonic region downstream of the Mach disk and supersonic region downstream of the oblique shock. In the latter region the periodic density variation is formed because the expansion waves induced by the interaction of oblique shock waves with jet boundary are reflected iteratively. Additionally, in Fig. 7(b) maximum pressure on the cone surface does not seem to be in the central region of the jet. For the flow field of the jet issuing from convergent nozzle with *NPR* = 4.0 impinging on the flat plate, the flow pattern similar to that is reported by Henderson, Bridges and Wernet (2005). In their study, it is also mentioned that a recirculation zone may occur in the subsonic region downstream of the Mach disk, but in this study the existence of it is not clear.

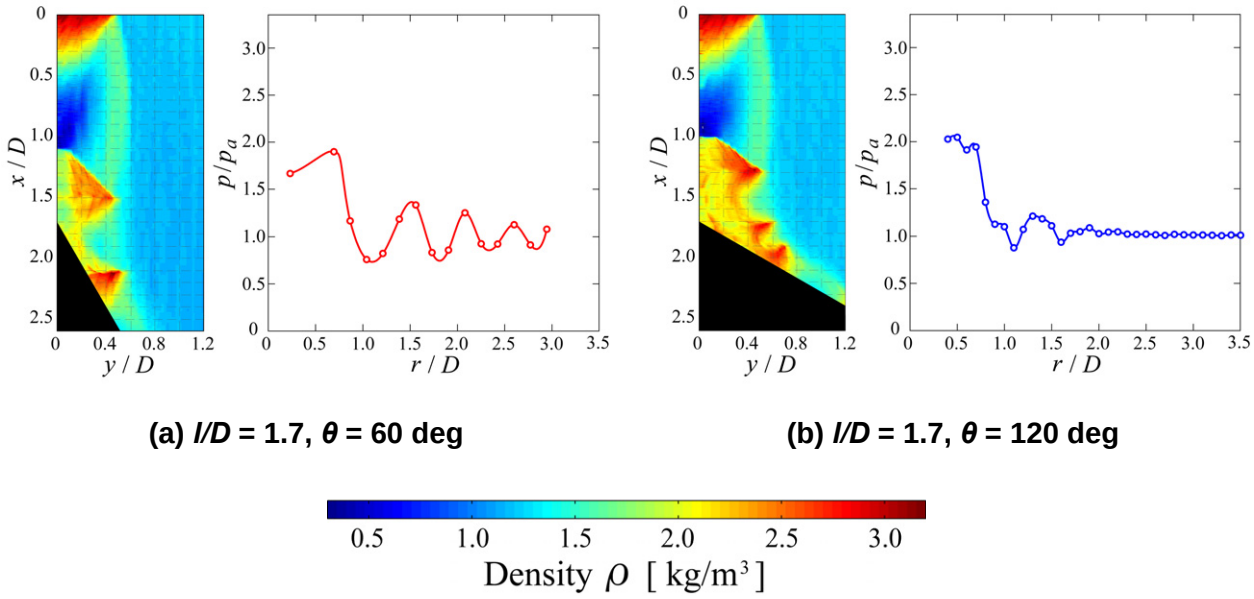

(a) *l*/*D* = 1.7, θ = 60 deg **(b) *l*/*D* = 1.7, θ = 120 deg**

Fig. 7. The density distributions obtained from interferograms (left side) and the pressure distributions on cone (right side) at *NPR* = 4.0

CONCLUSIONS

The flow field of the underexpanded jet impinging on cone is examined using the density distribution obtained by the Mach-Zehnder interferometry and the pressure distribution on the cone surface obtained by the pressure tap. For the *NPR* = 3.5, it is confirmed that depending on the vertex location in the cell structure of the free jet, the geometry and location of shock and the structure of the jet along the cone are changed, and as a result the flow patterns including the density distribution in the flow field and the pressure distribution on the cone surface are changed. It is also found that depending on the vertex angle, the flow pattern is clearly different. In comparison with the flow field at *NPR* = 4.0, having a Mach disk, and that at *NPR* = 3.5, not having a Mach disk, it is observed that the Mach disk changes the flow pattern and for this case the maximum pressure on the cone surface may not occur in the central axis.

ACKNOWLEDGMENTS

The experiments described above were made in cooperation with Y. Obuchi and Y. Kakurai. The authors would like to thank their assistances.

REFERENCES

B. Henderson (2002), "The connection between sound production and jet structure of the supersonic impinging jet", Journal of the Acoustical Society of America, **111**(2), 735–747.

B. Henderson, J. Bridges and M. Wernet (2005), "An experimental study of the oscillatory flow structure of tone-producing supersonic impinging jets", Journal of Fluid Mechanics, **542**, 115–137.

J. Iwamoto (1990), "Impingement of Under-Expanded Jets on a Flat Plate", Trans. ASME, Journal of Fluids Engineering, **112**, 179–184.

I. K. Jennions and B. L. Hunt (1980), "THE AXISYMMETRIC IMPINGEMENT OF SUPERSONIC AIR JETS OF CONES", Aeronautical Quarterly, **Feb.**, 26–39.

R. Ladenburg, J. Winckler and C. C. Van Voorhis (1948), "Interferometric Studies of Faster than Sound Phenomena. Part I. The Gas Flow around Various Objects in a Free, Homogeneous, Supersonic Air Stream", Physical Review, **73**(11), 1359–1377.

P. J. Lamont and B. L. Hunt (1976), "The impingement of underexpanded axisymmetric jets on wedges", Journal of Fluid Mechanics, **76**, 307–336.

T. Nakamura and J. Iwamoto (2000), "Experimental Study on Oscillation Mode of Underexpanded Impinging Jet and Behavior of Plate Shock Waves", Transactions of the Japan Society for Aeronautical and Space Sciences, **43**(141), 137–142.

J. Panda (1998), "Shock oscillation in underexpanded screeching jets", Journal of Fluid Mechanics, **363**, 173–198.

Christopher K. W. Tam (1995), "SUPERSONIC JET NOISE", Annual Review of Fluid Mechanics, **27**, 17–43.

APPENDIX I. NOTATION

The following symbols were used …

NPR	Ratio of stagnation pressure in the plenum tank to the atmospheric pressure
l	Nozzle-cone distance [mm]
D	Nozzle diameter [mm]
θ	Vertex angle of the cone [deg]
x	Axial coordinate [mm]
y	Radial coordinate [mm]
r	Distance measured from vertex of the cone along cone surface [mm]
p	Pressure on cone surface [Pa]
p_a	Atmospheric pressure [Pa]
ρ	Density [kg/m^3]